On-Line Testing of Lab-on-Chip Using Digital Microfluidic Compactors[1]

Yang Zhao and Krishnendu Chakrabarty
Department of Electrical and Computer Engineering
Duke University
Durham, NC 27708, USA
{yz61, krish}@ee.duke.edu

Abstract

Dependability is an important system attribute for microfluidic lab-on-chip devices. On-line testing offers a promising method for detecting defects, fluidic abnormalities, and bioassay malfunctions during chip operation. However, previous techniques for reading test outcomes and analyzing pulse sequences are cumbersome, sensitive to the calibration of capacitive sensors, and error-prone. We present a built-in self-test (BIST) method for on-line testing of digital microfluidic lab-on-chip. This method utilizes microfluidic compactors based on droplet-based AND gates, which are implemented using digital microfluidics. Dynamic reconfiguration of these compactors ensures low area overhead and it allows BIST to be interleaved with bioassays in functional mode.

1. Introduction

Microfluidic-based lab-on-chips are being advocated for applications such as immunoassays, clinical diagnosis and high-throughput DNA sequencing [1]. An especially promising technology platform is based on the principle of electrowetting-on-dielectric. Discrete droplets of nanoliter volumes can be manipulated in a "digital" manner under clock control on a two-dimensional array of electrodes ("unit cells"). Hence this technology is referred to as "digital microfluidics" [2].

An emerging application of microfluidics lies in the use of droplets for microfluidic computing. Microfluidic computing inherits the advantages of both microfluidics for sensing and computing for information processing [5]. It can potentially enhance microfluidic technology through direct incorporation of computing functions on-chip with other primary sensing functions. Digital microfluidics offers a promising enabling technique for on-chip logic functionality and for integrating sensing, computing, and on-line monitoring.

A prototype lab-on-chip has been developed for gene sequencing through synthesis [1], which targets the simultaneous execution of 106 fluidic operations and the processing of billions of droplets. Other lab-on-chip systems are being designed for protein crystallization, which requires the concurrent execution of hundreds of operations [17]. A commercially available droplet-based lab-on-chip embeds more than 600,000 20 μm by 20 μm electrodes with integrated optical detectors [8]. Recent years have therefore seen growing interest in design-automation and test techniques for the digital microfluidic platform [7, 10, 11, 14]. Test techniques for other microfluidic platforms have also been developed [4].

Microfluidics-based lab-on-chip devices are expected to be deployed for safety-critical biomedical applications such as point-of care diagnostics, health assessment and screening for infectious diseases. Therefore, dependability is an essential system attribute for lab-on-chip. An increase in the density and area of microfluidics-based lab-on-chip will lead to high defect densities, thereby reducing yield. These systems need to be tested adequately not only after fabrication, but also continuously during in-field operation. On-line testing, which allows testing and normal biochemical assays to run simultaneously on a microfluidic system, can therefore play an important role. It facilitates built-in self-test (BIST) of microfluidics-based lab-on-chip systems and makes them less dependent on costly manual maintenance on a regular basis.

A cost-effective test method for digital microfluidic systems was first described in [13]. Likely physical defects in such systems were analyzed and faults were classified as being either catastrophic or parametric. Further details on defects and fault models are presented in [15]. Faults can be detected by electrically controlling and tracking the motion of test droplets. In [12], a concurrent testing tech-

[1]This work was supported in part by the National Science Foundation under grant CCF-0541055.

978-0-7695-3264-6/08 $25.00 © 2008 IEEE
DOI 10.1109/IOLTS.2008.45

nique is presented for detecting catastrophic faults in digital microfluidics. A parallel scan-like testing methodology of structural test is proposed for digital microfluidic devices in [15]. A diagnosis method based on test outcomes has also been proposed to locate both single and multiple defect sites. In [16], several techniques are proposed for the functional testing of droplet-based microfluidic lab-on-chip. These techniques address fundamental biochip operations such as droplet dispensing, droplet transportation, mixing, splitting, and capacitive sensing.

Previous test methods for the digital microfluidic platform use capacitive-sensing circuits to read and analyze test outcomes [12, 15, 16]. After reading the test-outcome droplets in a consecutive manner, the capacitive sensing circuit generates a pulse-sequence corresponding to the detection of these droplets. This approach requires an additional step to analyze the pulse sequence to determine whether the microfluidic array-under-test is defective. The reading of test outcomes and the analysis of pulse sequences increase test time; the latter procedure is especially prone to errors arising from inaccuracies in sensor calibration. The complexity of the capacitive-sensing circuit and the need for pulse-sequence analysis make previously proposed testing methods less practical, especially for field operation.

In this paper, we propose an on-line testing method for digital microfluidic lab-on-chip. This method utilizes microfluidic compactors based on AND gates implemented using digital microfluidics. Using the principle of electrowetting-on-dielectric, we implement AND gate through basic droplet-handling operations such as transportation, merging, and splitting. The same input-output interpretation enables the cascading of gates for the implementation of additional logic functions. The microfluidic compactor can compress the test-outcome droplets into one droplet that can be detected using a simple photo-diode detector, thereby avoiding the need for a capacitive-sensing circuit and complicated pulse-sequence analysis. Dynamic reconfiguration of the microfluidic compactors allows on-line testing to be implemented with bioassays simultaneously, and ensures negligible area overhead.

The rest of the paper is organized as follows. Section 2 provides an overview of digital microfluidic platforms. In Section 3, we describe the operation of a microfluidic AND gate. In Section 4, we use these AND gates for on-line testing. A compactor is proposed to compress the test-outcome droplets for response evaluation. Dynamic reconfiguration is used to interleave on-line testing with normal bioassay operations. Finally, conclusions are drawn in Section 5.

2. Digital Microfluidic Platform

In digital microfluidics, droplets of nanoliter volumes (typically 300nL) are manipulated on a two-dimensional

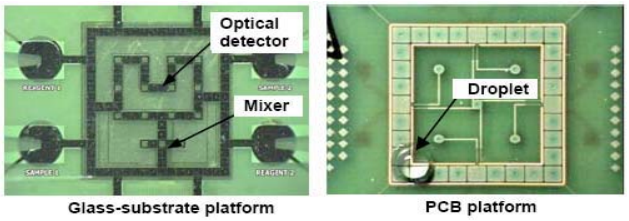

Figure 1. Fabricated digital microfluidic arrays [16].

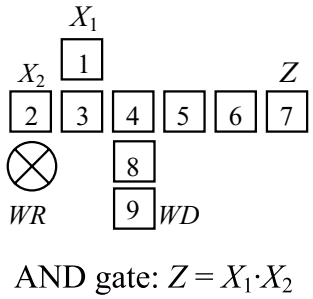

Figure 2. Schematic of microfluidic AND gate.

electrode array [1]. The typical size of the electrode is 1.5 $\times$ 1.5 mm^2. A unit cell in the array includes a pair of electrodes that acts as two parallel plates. The bottom plate contains a patterned array of individually controlled electrodes, and the top plate is coated with a continuous ground electrode. A droplet rests on a hydrophobic surface over an electrode, as shown in Fig. 1. Coplanar microfluidic arrays (without a top plate) have also been fabricated [6].

Droplets are moved by applying a control voltage to a unit cell adjacent to the droplet and, at the same time, deactivating the one under the droplet [3]. This electronic method of wettability control creates interfacial tension gradients that move the droplets to the charged electrode. Fluid-handling operations such as droplet merging, splitting, mixing, and dispensing can be executed in a similar manner. Droplet routes and operation schedules are programmed into a microcontroller that drives the electrodes.

3. Microfluidic AND Gate

In the digital microfluidic platform, droplets of unit volume (1x) or larger can be easily moved [3]. A droplet of 0.5x volume is not large enough to have sufficient overlap with an adjacent electrode; hence it cannot be moved with a nominal actuation voltage [3]. It has been verified experimentally that the times required for dispensing one droplet,

Table 1. Actuation-voltage sequence for the AND gate.

Clock cycle	Electrode No.								
	1	2	3	4	5	6	7	8	9
0	1	1	0	F	F	F	F	0	1
1	0	0	1	0	F	F	F	0	1
2	0	1	0	1	0	F	F	0	1
3	F	0	0	0	1	0	F	0	1
4	F	F	F	0	0	1	0	0	1
5	F	F	F	F	0	0	1	0	1

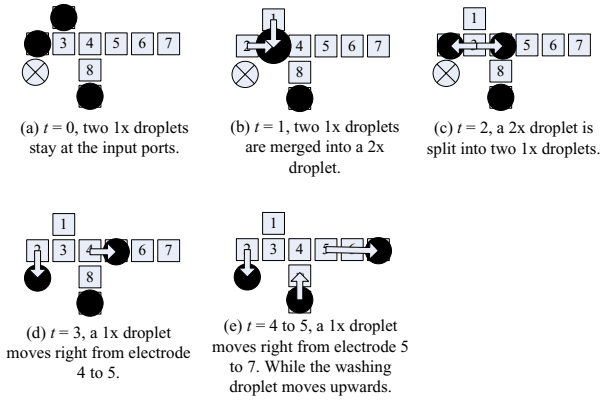

(a) t = 0, two 1x droplets stay at the input ports.

(b) t = 1, two 1x droplets are merged into a 2x droplet.

(c) t = 2, a 2x droplet is split into two 1x droplets.

(d) t = 3, a 1x droplet moves right from electrode 4 to 5.

(e) t = 4 to 5, a 1x droplet moves right from electrode 5 to 7. While the washing droplet moves upwards.

Figure 3. Operation of the AND gate with input 11.

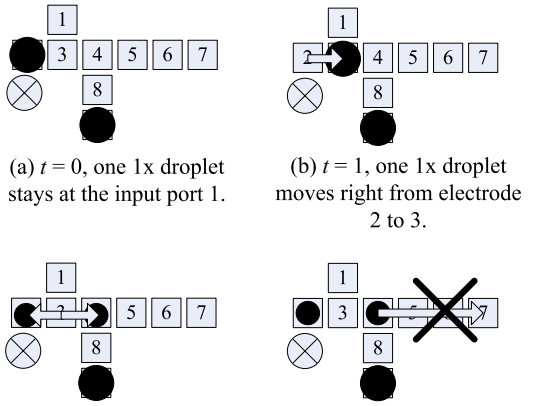

(a) t = 0, one 1x droplet stays at the input port 1.

(b) t = 1, one 1x droplet moves right from electrode 2 to 3.

(c) t = 2, a 1x droplet is split into two 0.5x droplets.

(d) t = 3 to 5, 0.5x droplet on electrode 4 cannot be moved to electrode 7.

Figure 4. Operation of the AND gate with input 01.

splitting a droplet into two, merging two droplets into one, and transporting a droplet to an adjacent electrode are nearly identical. This duration is defined as one time frame (clock cycle).

The definitions for logic values '0' or '1' are as follows: the presence of a droplet of 1x volume at an input or output port indicates a logic value of '1'. The absence of a droplet at an input or output port indicates the logic value '0'. The same interpretations at inputs and outputs enable the output of one gate to be fed as an input to another gate, thus logic gates can be easily cascaded.

Fig. 2 illustrates the schematic of a 2-input microfluidic AND gate. The AND gate incorporates a waste reservoir (WR) and nine indexed electrodes. Electrode 1 and Electrode 2 are the two input ports X_1 and X_2; Electrode 7 is the output port (Z). Electrode 9 is the washing port (WD).

The sequence of control voltages applied to each electrode is shown in Table 1. A '1' ('0') entry in the table indicates a high (low) voltage to the corresponding electrode in that clock cycle. An 'F' entry indicates a floating signal, i.e., the corresponding electrode is not required to be either high or low. The sequence of control voltages is independent of the input logic values.

Fig. 3 describes the cycle-by-cycle operation of the AND gate for $X_1X_2 = 11$. At clock cycle 0, two 1x droplets stay at two input ports (Electrode 1 and 2). At clock cycle 5, there is a 1x droplet on electrode 9, showing that the output value of this AND gate is 1.

Fig. 4 illustrates the cycle-by-cycle operation of the AND gate for $X_1X_2 = 01$. At clock cycle 0, one 1x droplet stays at the second input port (Electrode 2), while there is no droplet on the first input port (Electrode 1). At clock cycle 2, the 1x droplet on electrode 3 is split into two 0.5x droplets. The 0.5x droplet cannot be moved even if the adjacent electrode is activated at clock cycle 3. Therefore, at clock cycle 5, there is no droplet on electrode 7, showing that the output value of this AND gate is 0. Due to symmetry, $X_1X_2 = 10$ yields the same output value.

The delay of the AND gate is 5 clock cycles (or clock cycles), independent of the inputs. At the beginning of clock cycle 6, the droplet on the washing port (Electrode 9) is routed into the AND gate to clean the residuals and transport them to the waste reservoir.

We experimentally verified the functionality of the AND gate by configuring it on a fabricated lab-on-chip, then activating the corresponding electrodes to perform cycle-by-cycle operations. A typical experimental setup is shown in Fig. 5(a). The chip-under-test was mounted on a custom-assembled platform. We used a custom-made electronic unit to independently control the voltages of each control electrode in the array by switching them between ground and a DC actuation voltage. In our experiments, the actua-

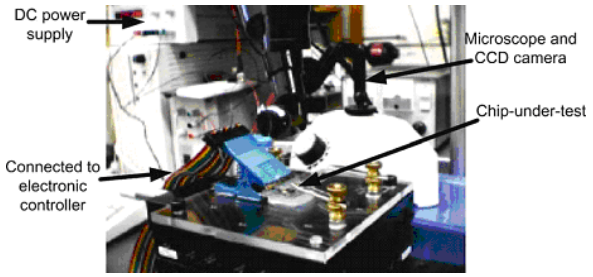

(a) Experimental setup [3]

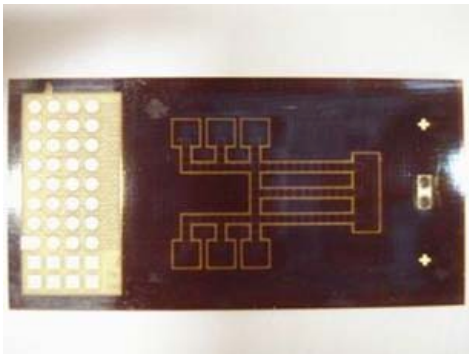

(b) Fabricated chip used for experiments

Figure 5. Experimental setup and fabricated lab-on-chip.

tion voltage was set to 50 V. The chip-under-test is a PCB microfluidic prototype for protein crystallization, as shown in Fig. 5(b).

4. Application to On-line Testing

In [12], a concurrent testing technique has been proposed for detecting catastrophic faults in digital microfluidic lab-on-chips. Multiple test droplets are routed in the microfluidic array at the same time when biochemical assays are executed; these test droplets traverse (cover) all the cells in the array. An integer linear programming model has been developed to derive an optimal droplet flow path for concurrent testing. Test plans are proposed to interleave test application with the set of biochemical assays to prevent the resource conflicts. This method offers an opportunity to implement BIST for microfluidic systems, and therefore eliminates the need for external test equipment.

Most catastrophic faults result in a complete cessation of droplet transportation. Thus, for the faulty system, the test droplet is stuck during its motion. However, for a fault-free system, all test droplets can be observed at the droplet sink by a capacitive-sensing circuit. Therefore, the fault-free or faulty status of a lab-on-chip can be easily determined by simply observing the arrival of test droplets at some selected ports of the system. However, in [12], each test droplet needs a sink reservoir, which complicates chip packaging and increases fabrication cost. An additional evaluation step is required to analyze the sequence of pulses generated by the capacitive-sensing circuit, to determine whether the microfluidic array-under-test has a defect. For example, if a unit cell of an array is faulty, no pulse is generated for the test droplet that covers the cell. Higher fabrication and packaging costs, the complexity of the capacitive-sensing circuit, and the need to analyze complex pulse is a major drawback of [12]. Moreover, there is a need to calibrate the pulse-analysis system and errors are likely due to the lack of a "noise margin".

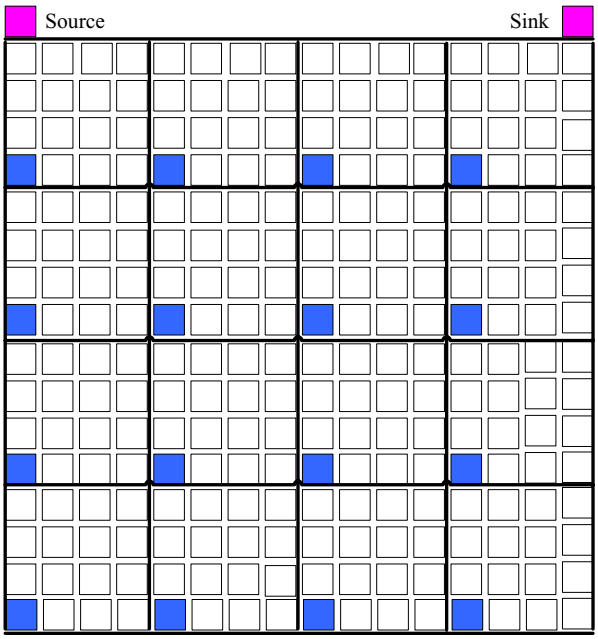

(a) Placement of a 16x16 microfluidic array

1	2	3	4	Row 1
5	6	7	8	Row 2
9	10	11	12	Row 3
13	14	15	16	Row 4

(b) Partition of a 16x16 microfluidic array

Figure 6. Placement and partition of a 16 $\times$ 16 microfluidic array.

To solve the above problems, we propose a microfluidic

compactor to compress multiple test-outcome droplets into one "signature" droplet during on-line testing. The signature droplet can be easily detected by a simple detector composed of a photo-diode and LED. The microfluidic compactor consists of a tree of logic AND operations implemented by 2-input microfluidic AND gates. Each input of the AND gates in the first layer is one of the test-outcome droplets. The outputs of these AND gates are used as the inputs of AND gates in the second layer. The output of the single AND gate in the last layer is connected to the photo-diode detector located at the sink of the microfluidic array. The compaction that is implemented by AND gates can be performed simultaneously with a normal biochemical assay by dynamically reconfiguring the cells that are available (not used by bioassays) at that time. Dynamic reconfiguration of the microfluidic compactors allows on-line testing to be interleaved with bioassays in functional mode.

For example, Fig. 6 shows how we perform concurrent testing with a microfluidic compactor for a 16 $\times$ 16 microfluidic array. Fig. 6(a) illustrates the placement of unit cells for the array. To simplify packaging and reduce fabrication cost, only one source reservoir and one sink reservoir with its photo-diode detector are included. The array is partitioned into sixteen non-overlapping parts, and the overall system can now be viewed as a 4 $\times$ 4 "macro" array; see Fig. 6(b). Each partition (referred to as a macro cell) consists of 4 $\times$ 4 unit cells.

Each macro cell has a test droplet located in the shaded cell in Fig. 6(a). The test droplets are preloaded into the macro cells before the start of the biochemical assay. Each test droplet can traverse all 16 cells in the macro cell to detect catastrophic faults when this macro cell is available (not used by the biochemical assay). The time needed for this droplet-traversed process in a macro cell is referred to as a macro-time frame. If there is no catastrophic fault in the macro cell, the corresponding test droplet will return to the shaded cell at the end of the macro-time frame; Otherwise, the test droplet will be stuck during its motion.

Table 2 presents the macro cells that are used for an example biochemical assay. On-line testing and droplet compaction are illustrated for each macro-time frame. C1, C2, ..., C16 represent the sixteen macro cells. The schedule for biochemical assays is presented in the second column of Table 2. At each macro-time frame, multiple macro cells are used for biochemical assays. The macro cells not involved in biochemical assays at that macro-time frame can be tested by the test droplets within them concurrently; see the third column of Table 2. Fig. 7 illustrates the schedule in Table 2 for biochemical assays and on-line testing of macro cells.

The compaction tree of logic AND operations is shown in Fig. 8. If the microfluidic array is fault-free, the sixteen test droplets can be compacted into one signature droplet.

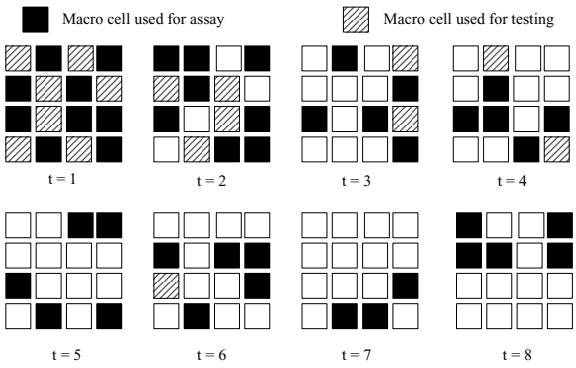

Figure 7. Schedule of biochemical assays and testing in a 16 $\times$ 16 microfluidic array.

Otherwise, if there is at least one catastrophic fault in the microfluidic array, the test droplets of the faulty macro cells are stuck during their motion, and the corresponding input values of the tree are '0'. So the output of the compaction tree is '0', indicating the faulty status.

The schedule of these AND operations is presented in the fourth column of Table 2. If two adjacent macro cells have already been tested in previous macro-time frames and are available in the current macro-time frame, the two test-outcome droplets can be compressed using an AND gate reconfigured within the two macro cells. If two AND operations targeting four macro cells in a row have been finished, and this row is available in the current macro-time frame, the two outcome droplets in this row can be further compressed into one droplet by an AND gate reconfigured within this row. For example, C6 and C5 are tested in the first and second macro-time frame, respectively, and they are available in macro-time frame 3, so the AND(C5, C6) operation can be implemented at this macro-time frame. At macro-time frame 5, AND(C5, C6) and AND(C7, C8) have been implemented in macro-time frame 3 and 4 respectively, and row 2 including C5 to C8 is available, so the AND(Row 2) operation can be implemented. The schedule in Table 2 interleaves the bioassays, concurrent on-line testing, and test-outcome compaction, and prevents resource conflicts.

As shown in Table 2, the concurrent testing of the microfluidic array is finished in 6 macro-time frames, and the compaction of the test-outcome droplets is finished in 10 macro-time frames. Instead of routing all test-outcome droplets serially to a capacitive-sensing circuit connected to the sink reservoir for pulse-sequence analysis, we move the signature droplet after compaction to the photo-diode detector.

Table 2. Schedule of biochemical assay, testing steps and compaction steps in a 16 $\times$ 16 microfluidic array.

Macro-time frame	Macro cells used for assay	Macro cells used for testing	Compaction operations
1	C2,C4,C5,C7,C9,C11,C12,C14,C16	C1,C3,C6,C8,C10,C13,C15	
2	C1,C2,C4,C6,C9,C12,C15,C16	C5,C7,C11,C14	
3	C2,C8,C9,C11,C16	C4,C12	AND(C5,C6), AND(C13,C14)
4	C6,C9,C10,C12,C15	C2,C16	AND(C7,C8), AND(C3,C4)
5	C3,C4,C9,C14,C16		AND(C1,C2), AND(C11,C12), AND(Row2)
6	C5,C7,C8,C12,C14	C9	AND(C15,C16), AND(Row1)
7	C12,C14,C15		AND(C9,C10), AND(Row1,Row2)
8	C1,C4,C5,C6,C8		AND(Row3), AND(Row4)
9			AND(Row3,Row4)
10			AND(Row1&2,Row3&4)

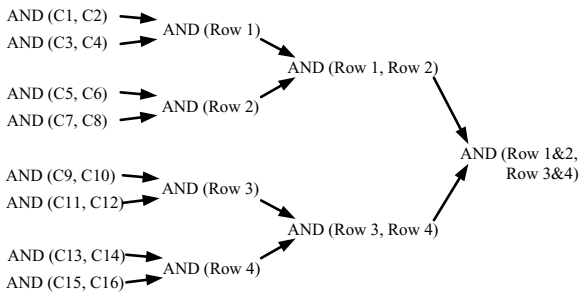

Figure 8. Schematic of a microfluidic compactor for concurrent testing.

5. Conclusion

We have presented an on-line testing method for digital microfluidic lab-on-chip. This method utilizes digital microfluidic AND gates to implement a compactor for mapping multiple test-outcome droplets to a signature droplet. The AND gate is implemented using the principle of electrowetting-on-dielectric. The microfluidic compactors obviate the need for error-prone multiple capacitive-sensing circuits. Dynamic reconfiguration of the microfluidic compactors allows both on-line testing and biochemical assays to be implemented concurrently, and ensures low area overhead.

References

[1] R. B. Fair et al., "Chemical and biological applications of digital-microfluidic devices", *IEEE Design & Test of Computers*, vol. 24, pp. 10-24, 2007.

[2] K. Chakrabarty and F. Su, *Digital Microfluidic Biochips: Synthesis, Testing, and Reconfiguration Techniques*, CRC Press, Boca Raton, FL, 2006.

[3] M. G. Pollack, *Electrowetting-Based Microactuation of Droplets for Digital Microfluidics*, PhD thesis, Duke University. 2001.

[4] H. G. Kerkhoff, "Testing microelectronic biofluidic systems", *IEEE Design & Test of Computers*, vol. 24, pp. 72-82, 2007.

[5] D. W. M. Marr and T. Munakata, "Micro/Nanofluidic computing", *Comm. ACM*, vol. 50, pp. 64-68, 2007.

[6] P. Paik, V. K. Pamula, M. G. Pollack, and K. Chakrabarty, "Coplanar Digital Microfluidics Using Standard Printed Circuit Board Processes," *Proc. Micro Total Analysis Systems*, 2005.

[7] A. J. Ricketts, K. Irick, N. Vijaykrishnan, and M. J. Irwin, "Priority scheduling in digital microfluidics-based biochips", *Proc. DATE Conf.*, pp. 329-334, 2006.

[8] Silicon Biosystems. www.siliconbiosystems.com

[9] V. Srinivasan, V. K. Pamula, M. G. Pollack and R. B. Fair, "Clinical diagnositics on human whole blood, plasma, serum, urine, saliva, sweat, and tears on a digital microfluidic platform", *Proc. Micro Total Analysis Systems*, pp. 1287-1290, 2003.

[10] F. Su, W. Hwang, A. Mukherjee and K. Chakrabarty, "Testing and diagnosis of realistic defects in digital microfluidic biochips", *JETTA*, vol. 23, pp. 219-233, 2007.

[11] F. Su, K. Chakrabarty and R. B. Fair, "Microfluidics-based biochips: technology issues, implementation platforms, and design automation challenges", *IEEE Trans. CAD*, vol. 25, pp. 211-223, 2006.

[12] F. Su, S. Ozev and K. Chakrabarty, "Concurrent testing of droplet-based microfluidic systems for multiplexed biomedical assays", *Proc. Int. Test Conf.*, pp. 883-892, 2004.

[13] F. Su, S. Ozev and K. Chakrabarty, "Testing of droplet-based micro-electrofluidic systems", *Proc. Int. Test Conf.*, pp. 1192-1200, 2003.

[14] P. H. Yuh, C. L. Yang, and C. W. Chang, "Placement of defect-tolerant digital microfluidic biochips using the T-tree formulation", *ACM J. Emerging Tech. Computing Sys.*, vol. 3, pp. 13.1-13.32, 2007.

[15] T. Xu and K. Chakrabarty, "Parallel scan-like test and multiple-defect diagnosis for digital microfluidic biochips", *IEEE Trans. Biomedical Circuits and Sys.*, vol. 1, pp. 148-158, 2007.

[16] T. Xu and K. Chakrabarty, "Functional testing of digital microfluidic biochips", *Proc. Int. Test Conf.*, 2007.

[17] T. Xu, P. Thwar, V. Srinivasan, V. K. Pamula, and K. Chakrabarty, "Digital microfluidic biochip for protein crystallization", *IEEE-NIH Life Science Systems and Applications Workshop*, Bethesda, MD, 2007.